

# AIR TEMPERATURE ANALYSIS AND CONTROL IMPROVEMENT FOR THE LARGE-SCALE EXPERIMENTAL HALL

J.C. Chang<sup>a, d</sup>, M.T. Ke<sup>b</sup>, C.Y. Liu<sup>a</sup>, and J. R. Chen<sup>a, c</sup>

<sup>a</sup>National Synchrotron Radiation Research Center (NSRRC), Hsinchu 300, Taiwan

<sup>b</sup>Graduate Institute of Air-Conditioning and Refrigeration Engineering, National Taipei University of Technology, Taipei 106, Taiwan

<sup>c</sup>Department of Nuclear Science, National Tsing-Hua University, Hsinchu 300, Taiwan

<sup>d</sup>E-Mail: jcchang@nsrrc.org.tw

## Abstract

This paper presents the air temperature analysis and control improvement for the large-scale experimental hall, in which twenty-six beamlines currently located, at the Taiwan Light Source (TLS). The inner and outer diameters and height of the donut-shaped experimental hall are 29m, 80m and 11.7m, respectively. Totally seventy-two temperature sensors are installed in this zone, where sixty sensors are installed along the beamlines, to on-line record the air temperature history. Because of lack of cooling capacity and poor design of air-conditioning (A/C) system, the air temperature variation may be more than 2 °C in one day. The temperature difference between different beamlines is also about 2 °C. To cope with those problems, a computational fluid dynamics (CFD) code is applied to simulate the spatial temperature variation. The A/C supply air outlet and exhaust locations will then be optimum rearranged according to the CFD simulation results.

## INTRODUCTION

The TLS has made many efforts on studying the utility effect on beam quality and upgrading utility conditions since 1998 [1][2]. These studies show that the stability of the electron beam orbit is sensitive to the thermal effects, whose propagation routes from the temperature variation to the beam quality are also tracked. Some detailed thermal effect studies and A/C system improvements were conducted afterward, including the CFD simulation for the air-cooling magnet lattice girder [3] and the mini environment control for the elliptical polarization undulator [4]. We also made much improvement on air temperature control for the storage ring tunnel in 2003 [5]. The air temperature variation in the storage ring tunnel is globally controlled within  $\pm 1^\circ\text{C}$  currently.

However, the cooling capacity of the storage experimental hall becomes more insufficient than ever. There were originally total four air handling units (AHU), whose specifications are shown in Table 1, serving for two main areas of the storage ring building, i.e., the storage ring tunnel and the experimental hall. Last year's A/C system modification [5] had increased the cooling capacity of the storage ring tunnel but decreased that of the experimental hall. Besides, all the A/C ventilation inlets are distributed on the ceiling and the outlets are located in the inner ring, and all are high above the

beamlines in the experimental hall. The poor air supply air outlet and exhaust arrangement results in the supply air a shortcut path and worsens the cooling efficiency. The temperature distribution analysed by CFD simulation will be shown in the later section.

Accordingly, a series of field measures are performed to collect the air and beamlines temperature. The cooling capacity is estimated and the temperature and flow field of the experimental hall are simulated to propose an optimal A/C system improvement retrofit plan.

Table 1: Specifications of the AHU for the storage ring.

Air flow (cfm)	Fan (RPM)	Fan static pressure (in WG)	Motor (HP)	Cooling water flow rate (GPM)
12800	1962	3.5	20	80

## TEMPERATURE MEASUREMENT AND COOLING LOAD ESTIMATION

There are total twenty-six beamlines and forty-nine end stations are located in the experimental hall currently. The first step to control the air temperature in this area is to record the temperature history. We install two to five temperature sensors on some critical position of specific beamline, as shown in Figure 1. Those temperature sensors are numbered on Figure 1. Twelve temperature sensors are installed on the outer wall of the experimental hall. The temperature histories of these seventy-two locations are on-line recorded on the archive system.

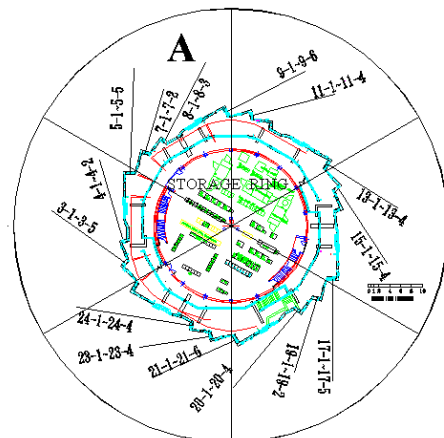


Figure 1: Storage ring layout and temperature sensors distribution.

Figure 2 shows one week's outdoor atmosphere and indoor air temperature histories on two different locations in the experimental hall. It was recorded last summer. The highest outdoor atmosphere temperature is 33 °C or so. The outdoor and indoor air temperature variations during one day are about 8 °C and 2 °C, respectively. The cooling capacity was fully loaded and showed obviously insufficient. The air temperature difference between two different locations is also about 2 °C.

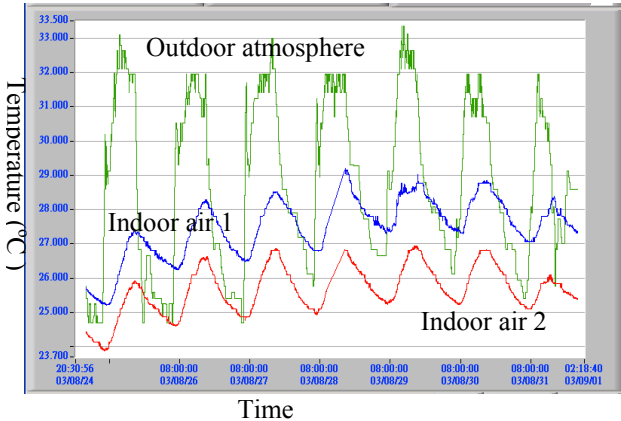


Figure 2: Outdoor atmosphere and indoor air temperature histories.

We estimate the cooling load according to the current experimental hall conditions. The major thermal loading is divided as four parts, namely, ceiling heat load, internal equipment heat load dissipated, human heat load and ventilation load. The thermal effects of solar radiation and the indoor and outdoor temperature difference are taken into consideration in estimating the ceiling load, and the calculation is referred to ASHRAE Handbook Fundamentals [6]. The estimated results are listed in Table 2 and serve as the boundary conditions for the CFD simulation.

### NUMERICAL ANALYSIS AND SIMULATION

We use FLUENT 6.1, a CFD code, to perform the numerical simulation. About four million grids are generated to simulate the whole area. Such a large-scale simulation will make the computation consume too much memory and take too much time. To cope with this problem, we divide the experimental hall as periodically symmetric six sections, as shown in Figure 1 and assume periodic boundary condition for each section. Accordingly, we may simplify the simulation by only simulating any one of these six sections then applying the results to other five sections. We choose section A, as shown in Figure 1, to model and simulate. The three dimensional model of this section is shown in Figure 3.

As shown in Figure 3, brown spots on the ceiling and blue rectangles on the inner wall are air outlets and exhausts, respectively. Total 629,524 tetrahedron grids with 0.32m-edge are generated in the simulated area. The boundary conditions are listed in Table 2.

Table 2: Boundary conditions for CFD simulation.

Air outlet (On the ceiling)	Wind velocity	1.34 m/s
	Temperature	14.2 °C
Ceiling heat flux		55.7 W/m <sup>2</sup>
Heat source	Beamline and human	1.68 W/m <sup>3</sup>
Wall and floor		Adiabatic

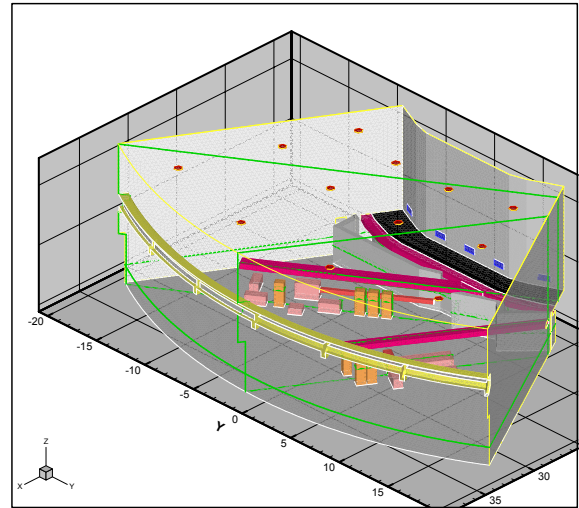


Figure 3: Physical model of simulation for current experimental hall.

Figure 4 shows the simulated temperature field for current experimental hall. Two red thin zones on top of two cross-sections demonstrate high temperature resulted from the ceiling heat flux. Because the air outlets are designed on the ceiling, the temperature of upper zone is lower. On the contrary, the temperature of the area near beamlines is higher due to the heat source of beamlines, as shown in the figure. This two-layer temperature distribution demonstrates the inefficient A/C ventilation design.

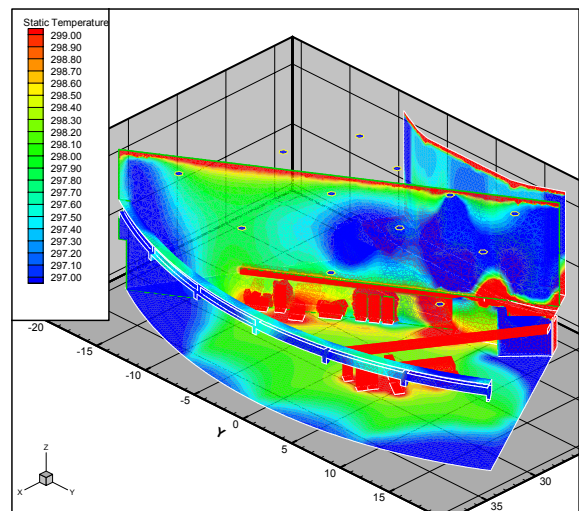


Figure 4: Simulated temperature field for current experimental hall.

## A/C SYSTEM IMPROVEMENT PLAN

Because of abovementioned current insufficient cooling capacity and inefficient A/C ventilation design, an A/C system improvement plan for the experimental hall is necessary. We thus design a new improved A/C system as shown in Figure 5.

As shown in Figure 5, three new AHUs, represented by blue cuboids, are added in the A/C system outside the experimental hall. The total cooling capacity will also be increased about three times the current capacity. The supplied air duct is designed on the outer wall, where the blue circular duct located in Figure 5. Three return air ducts are respectively connected to AHUs and core area, which serves as a return air box. Air supply outlets and exhausts are designed on the supplied air duct and the inner wall of the experimental.

The flow rate of the supply air will be increased. The angle of depression of the ventilation inlet is adjustable to make supplied air efficiently and uniformly flow through the whole experimental.

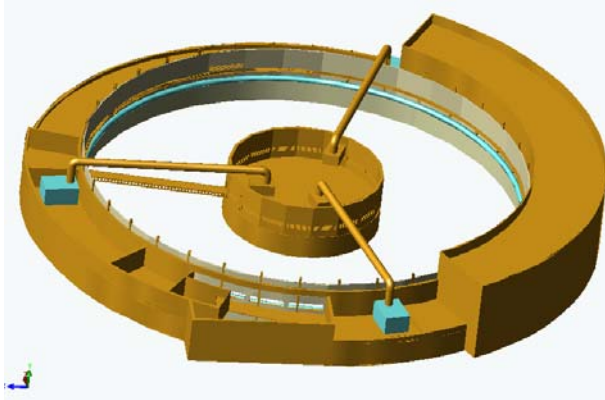


Figure 5: A/C system improvement design.

We also simulate the flow field of the experimental hall with the improved A/C system. The boundary conditions are kept the same as those listed in Table 2 except the air supply outlet, whose location is changed from the ceiling to the outer wall. And the supply air velocity is increased to 5.83 m/s and the temperature is 23 °C. The simulation result of the temperature field is shown in Figure 6. The low temperature area near supply air outlet indicates that the supplied air is not totally diffused yet there. However, the overall spatial temperature uniformity is obviously improved than that shown in Figure 4.

The improved A/C system construction is scheduled on the end of 2004.

## CONCLUSION

The cooling capacity of current A/C system for the experimental hall is estimated insufficient and verified by the air temperature measurement. The air temperature variation may be more than 2 °C during one day. The temperature difference between different beamlines is also about 2 °C. The current distribution of air outlet and exhaust generates the supply air shortcut and worsens the cooling efficiency.

CFD simulation for the experimental hall under current A/C condition is performed. Simulation result demonstrates the inefficient A/C ventilation design. A new improved A/C system is then designed and the flow field is simulated. The cooling capacity will be increased three times and the spatial air temperature uniformity will be much improved.

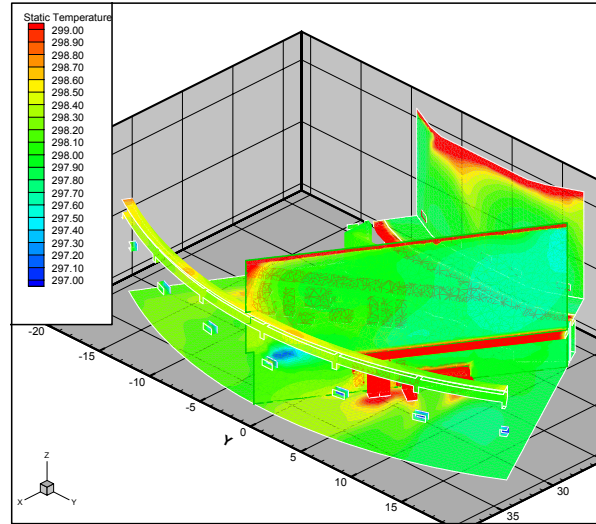


Figure 6: Simulated temperature field for the experimental hall with improved A/C system.

## REFERENCE

- [1] J.R. Chen, H.M. Cheng, Z.D. Tsai, C.R. Chen, T.F. Lin, G.Y. Hsiung, and Y.S. Hong, "The Correlation between the Beam Orbit stability and the Utilities at SRRC", Proc. of 6th European Particle and Accelerator Conference EPAC98, Stockholm, Sweden, June 22-26, 1998.
- [2] J.R. Chen, D.J. Wang, Z.D. Tsai, C.K. Kian, S.C. Ho, and J.C. Chang, "Mechanical Stability Studies at the Taiwan Light Source", 2nd Int'l Workshop on Mechanical Engineering Design of Synchrotron Radiation Equipment and Instrumentation (MEDSI02), APS, U.S.A., Sep 5-6, 2002.
- [3] D.S. Lee, Z.D. Tsai, J.R. Chen and C. R. Chen, "Cooling Air Flow Induced Thermal Deformation of the Magnet Lattice Girder", Proceedings of European Particle Accelerator Conference EPAC2000, Vienna, Austria, June 26-30, 2000.
- [4] D.S. Lee, Z.D. Tsai, and J.R. Chen, "Mini Environment Control for the Elliptical Polarization Undulator" 2001 Particle and Accelerator Conference (PAC), June 18-22, 2001, Chicago, USA.
- [5] J.C. Chang, C.Y. Liu, and J.R. Chen, "Air Temperature Control Improvement for the Storage Ring Tunnel" 2003 Particle and Accelerator Conference (PAC), May 12-16, 2003, Portland, USA.
- [6] ASHRAE Handbook, Fundamentals, Chapter 28, 2001.